Inorg. Chem. **2002**, *41*, 2616–2622

Pyridylazole Chelation of Oxorhenium(V) and Imidorhenium(V). Rates and Trends of Oxygen Atom Transfer from $Re^{V}O$ to Tertiary Phosphines

Jaydip Gangopadhyay,[†] Suman Sengupta,[†] Sibaprasad Bhattacharyya,[†] Indranil Chakraborty,[†] and Animesh Chakravorty*[,†,‡]

Department of Inorganic Chemistry, Indian Association for the Cultivation of Science, Kolkata 700 032, India, and Jawaharlal Nehru Centre for Advanced Scientific Research, Bangalore 560 064, India

Received October 15, 2001

The concerned azoles are 2-(2-pyridyl)benzoxazole (pbo) and 2-(2-pyridyl)benzthiazole (pbt). These react with $ReOCl_3(PPh_3)_2$ in benzene, affording $Re^{V}OCl_3$(pbo) and $Re^{V}OCl_3$(pbt), which undergo facile oxygen atom transfer to PPh_2R (R = Ph, Me) in dichloromethane solution, furnishing $Re^{III}(OPPh_2R)Cl_3$(pbo) and $Re^{III}(OPPh_2R)Cl_3$(pbt). The oxo species react with aniline in toluene solution, yielding the imido complexes $Re^{V}(NPh)Cl_3$(pbo) and $Re^{V}(NPh)Cl_3$(pbt). The X-ray structures of pbt, $ReOCl_3$(pbt), $Re(OPPh_3)Cl_3$(pbt), and $Re(NPh)Cl_3$(pbo) are reported. The lattice of pbt consists of stacked dimers. In all the complexes the azole ligand is N,N-chelated and the $ReCl_3$ moiety is meridionally disposed. In $ReOCl_3$(pbt) the metal–oxo bond length is 1.607(9) Å. The second-order rates and the associated activation parameters of the oxygen atom transfer reactions of the $Re^{V}O$ chelates with PPh_2R are reported. The large and negative entropy of activation (~ -24 eu) is consistent with an associative pathway involving nucleophilic phosphine attack. The rate increases with phosphine basicity ($PPh_2Me > PPh_3$) and azole heteroatom electronegativity (O(pbo) > S(pbt)). Logarithmic rate constants for $ReOCl_3$(pbo), $ReOCl_3$(pbt), and $ReOCl_3$(pal) are found to correlate linearly with $Re^{VI}O/Re^{V}O$ reduction potentials (pal is pyridine-2-(*N*-*p*-tolyl)aldimine). The relatively low rate constant of $ReOCl_3$(pbt) compared to that of $ReOCl_3$(pal) is consistent with the observed shortness of the metal–oxo bond in the former. Crystal data are as follows: (pbt) empirical formula $C_{12}H_8N_2S$, crystal system orthorhombic, space group $Pca2_1$, $a = 13.762(9)$ Å, $b = 12.952(8)$ Å, $c = 11.077(4)$ Å, $V = 1974(2)$ Å^3, $Z = 8$; ($ReOCl_3$(pbt)) empirical formula $C_{12}H_8Cl_3N_2OSRe$, crystal system monoclinic, space group $P2_1/c$, $a = 11.174(7)$ Å, $b = 16.403(10)$ Å, $c = 7.751(2)$ Å, $\beta = 99.35(4)°$, $V = 1401.8(13)$ Å^3, $Z = 4$; ($Re(NPh)Cl_3$(pbo)) empirical formula $C_{18}H_{13}Cl_3N_3ORe$, crystal system monoclinic, space group $P2_1/c$, $a = 9.566(6)$ Å, $b = 16.082(8)$ Å, $c = 11.841(5)$ Å, $\beta = 94.03(4)°$, $V = 1817(2)$ Å^3, $Z = 4$.

Introduction

This work stems from our interest in the design of new oxorhenium(V) reagents based on pyridyl ligands and in the chemical transformations thereof providing access to other rhenium systems.[1−3] A notable reaction of $Re^{V}O$ species is oxygen atom transfer to oxophilic substrates.[1−7] Transfer reactions promoted by enzymatic oxo sites based on iron, molybdenum, and tungsten are important in the chemistry of life.[8] Rhenium is not a biometal in the same sense, but as an element in the periodic group next to that of molybdenum and tungsten, transfer reactions involving $Re^{V}O$ are of value as potential models.[3]

In the pyridyl ligands used so far (pyridine-2-aldimines are representative examples), N,N-chelation of $Re^{V}O$ is completed by the pyridine nitrogen along with a nitrogen site present in an acyclic substituent pendent from the

* To whom correspondence should be addressed at the Indian Association for the Cultivation of Science. Fax: +91-33-473-2805. E-mail: icac@mahendra.iacs.res.in.

[†] Indian Association for the Cultivation of Science.

[‡] Jawaharlal Nehru Centre for Advanced Scientific Research.

(1) Banerjee, S.; Bhattacharyya, S.; Dirghangi, B. K.; Menon, M.; Chakravorty, A. *Inorg. Chem.* **2000**, *39*, 6 and references therein.

(2) (a) Chakraborty, I.; Bhattacharyya, S.; Banerjee, S.; Dirghangi, B. K.; Chakravorty, A. *J. Chem. Soc., Dalton Trans.* **1999**, 3747. (b) Bhattacharyya, S.; Chakraborty, I.; Dirghangi, B. K.; Chakravorty, A. *Inorg. Chem.* **2001**, *40*, 286. (c) Bhattacharyya, S.; Chakraborty, I.; Dirghangi, B. K.; Chakravorty, A. *J. Chem. Soc., Chem. Commun.* **2000**, 1813. (d) Menon, M.; Pramanik, A.; Das, S.; Bag, N.; Chakravorty, A. *Inorg. Chem.* **1994**, *33*, 403. (e) Menon, M.; Chowdhury, S.; Pramanik, A.; Deb, A. K.; Chandra, S. K.; Bag, N.; Goswami, S.; Chakravorty, A. *J. Chem. Soc., Chem. Commun.* **1994**, 57.

10.1021/ic011064t CCC: $22.00
Published on Web 04/11/2002

2-position of the pyridine ring.[1−3] The use of heterocyclic substituents instead would add a new dimension to pyridyl−$Re^{V}O$ chemistry. A familiar example of such a ligand is 2,2′-bipyridine, but the oxygen transfer behavior of its monooxo complexes such as $ReOCl_3(bpy)$[5,9] and $ReOMe_2(bpy)Cl_3$[9c] have not been documented. This has prompted us to explore other heterocyclic systems as possible ligands. Herein we report the synthesis and characterization of $Re^{V}O$ complexes incorporating chelation by 2-(2-pyridyl)azoles. Structure determination in one case has revealed the presence of a relatively short metal−oxo bond. The oxo chelates react with tertiary phosphines, furnishing stable phosphine oxide species. The rates and activation parameters of oxygen atom transfer are reported, and reactivity trends are scrutinized in terms of ligand variation, reduction potentials, and bond parameters. The $Re^{V}NPh$ species derived from the $Re^{V}O$ complexes are also reported, and the chelation mode of a hitherto unreported pyridyloxazole is authenticated by structure determination in one case.

Results and Discussion

Syntheses of Ligands and Complexes. The concerned ligands are 2-(2-pyridyl)benzoxazole (pbo) and 2-(2-pyridyl)-benzthiazole (pbt). To our knowledge pbo is a hitherto unreported oxazole. It has been synthesized in excellent yields by extending a procedure[10] based on the oxidation of Schiff bases by Ag_2O. A synthesis of pbt simpler than those reported[11] is described.

Upon reaction of $ReOCl_3(PPh_3)_2$ with the azoles in equimolar proportions in benzene at room temperature, the oxo complexes of type **1** are obtained as yellow solids, eq 1. Use of dichloromethane as the solvent (in which **1** is soluble) in the above synthesis leads to further reaction, eq 2, furnishing violet-colored complexes of type **2** (R = Ph) which can also be synthesized from preisolated **1** and PPh_3. The type **2** (R = Me) species were prepared from **1** and PPh_2Me. The blue-colored imide complexes of type **3** were synthesized by reacting **1** with excess aniline in toluene, eq 3.

$$ReOCl_3(PPh_3)_2 + \text{pbo/pbt} \rightarrow \mathbf{1} + 2PPh_3 \quad (1)$$

$$\mathbf{1} + PPh_2R \rightarrow \mathbf{2} \quad (2)$$

$$\mathbf{1} + PhNH_2 \rightarrow \mathbf{3} + H_2O \quad (3)$$

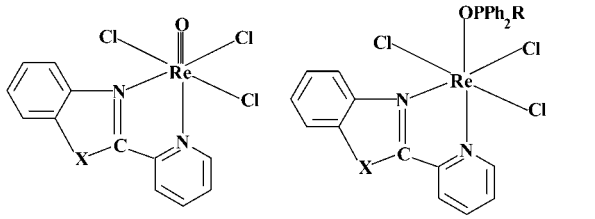

X = O , $ReOCl_3$(pbo)

X = S, $ReOCl_3$(pbt)

1

X = O , $Re(OPPh_2R)Cl_3$(pbo)

X = S, $Re(OPPh_2R)Cl_3$(pbt)

2

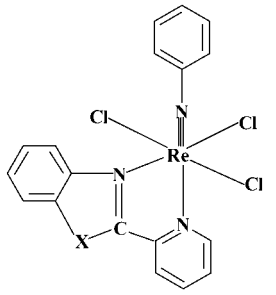

X = O, $Re(NPh)Cl_3$(pbo)

X = S, $Re(NPh)Cl_3$(pbt)

3

Selected characterization data for the ligands and complexes are given in the Experimental Section. The electronic spectra of the complexes are of diagnostic value and have been employed in rate studies (see below). The complexes of types **1** and **3** are diamagnetic ($5d_{xy}^2$) and give rise to normal ^1H NMR spectra. The type **2** complexes (t_{2g}^4) have magnetic moments near 2 μ_B as in some other rhenium(III) species, and their ^1H NMR spectra are paramagnetically shifted.[1,2,12]

Structures. The following compounds afforded single crystals and were subjected to X-ray crystallography: pbt, $ReOCl_3$(pbt), $Re(OPPh_3)Cl_3$(pbt), and $Re(NPh)Cl_3$(pbo). Satisfactory refinement could not be achieved in the case of $Re(OPPh_3)Cl_3$(pbt) due to crystallographic complications (see the Experimental Section). However, the results demonstrate beyond doubt that the overall connectivity is as in **2**.

A molecular view of pbt and selected bond parameters therein are shown in Figure 1. The asymmetric unit consists of two approximately planar (mean deviation ~0.05 Å) molecules lying parallel to each other in an eclipsed configuration. The distance between the centroids of the two molecules is 3.838(3) Å. Aromatic stacking is a general feature of all the structures reported here. The relative orientations of the azole molecules in the stacks, however, vary from one case to another.

(3) Dirghangi, B. K.; Menon, M.; Pramanik, A.; Chakravorty, A. *Inorg. Chem.* **1997**, *36*, 1095.
(4) Rowbottom, J. F.; Wilkinson, G. *J. Chem. Soc., Dalton Trans.* **1972**, 826.
(5) Bryan, J. C.; Stenkamp, R. E.; Tulip, T. H.; Mayer, J. M. *Inorg. Chem.* **1987**, *26*, 2283.
(6) Fontaine, X. L. R.; Fowles, E. H.; Layzell, T. P.; Shaw, B. L.; Thornton-Pett, M. *J. Chem. Soc., Dalton Trans.* **1991**, 1519.
(7) Seymore, S. B.; Brown, S. N. *Inorg. Chem.* **2000**, *39*, 325.
(8) (a) Hille, R. *Chem. Rev.* **1996**, *96*, 2757. (b) Holm, R. H. Kennepohl, P.; Solomon, E. I. *Chem. Rev.* **1996**, *96*, 2239.
(9) (a) Chakravorti, M. C. *J. Inorg. Nucl. Chem.* **1975**, *37*, 1991. (b) Fortin, S.; Beauchamp, A. L. *Inorg. Chem.* **2000**, *39*, 4886. (c) Jung, J. H.; Albright, T. A.; Hoffman, D. M.; Lee, T. R. *J. Chem. Soc., Dalton. Trans.* **1999**, 4487. (d) Ram, M. S.; Johnson, C. S.; Blackbourn, R. L.; Hupp, J. T. *Inorg. Chem.* **1990**, *29*, 238. (e) Fergusson, J. E. *Coord. Chem. Rev.* **1966**, 459 and references therein.
(10) Yoshifuji, M.; Nagase, R.; Kawashima, T.; Inamoto, N. *Heterocycles* **1978**, *10*, 57.
(11) (a) Miller, P. E.; Oliver, G. L.; Dann, J. R.; Gates, J. W. *J. Org. Chem.* **1957**, *22*, 664. (b) Lindoy, L. F.; Livingstone, S. E. *Inorg. Chim. Acta* **1967**, 365.
(12) (a) Bhattacharyya, S.; Banerjee, S.; Dirghangi, B. K.; Menon, M.; Chakravorty, A. *J. Chem. Soc., Dalton Trans.* **1999**, 155. (b) Gunz, H. P.; Leigh, G. J. *J. Chem. Soc. A* **1971**, 2229. (c) Tisato, F.; Refosco, F.; Bolzati, C.; Cagnolini, A.; Galto, S.; Bandoli, G. *J. Chem. Soc., Dalton Trans.* **1997**, 1421.

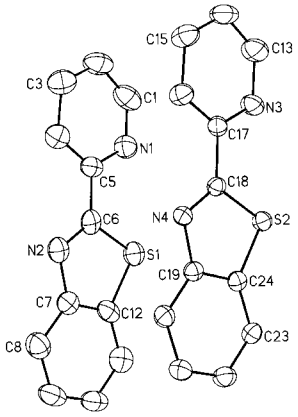

Figure 1. Molecular view and atom-labeling scheme for free pbt, **1**. All non-hydrogen atoms are represented by 30% thermal probability ellipsoids. Selected bond distances (Å) and angles (deg): C(18)−S(2) 1.728(6), S(2)−C(24) 1.719(6), C(24)−C(19) 1.399(8), C(19)−N(4) 1.365(7), N(4)−C(18) 1.282(7), C(6)−S(1) 1.728(8), S(1)−C(12) 1.733(7), C(12)−C(7) 1.371-(11), C(7)−N(2) 1.402(9), N(2)−C(6) 1.269(9); C(6)−S(1)−C(12) 89.1-(4), N(2)−C(6)−S(1) 116.8(6), S(1)−C(12)−C(7) 108.6(6), C(12)−C(7)−N(2) 115.8(7), C(7)−N(2)−C(6) 109.7(6), C(18)−S(2)−C(24) 88.6(3), N(4)−C(18)−S(2) 116.3(4), S(2)−C(24)−C(19) 109.4(4), C(24)−C(19)−N(4) 114.6(5), C(19)−N(4)−C(18) 111.0(5).

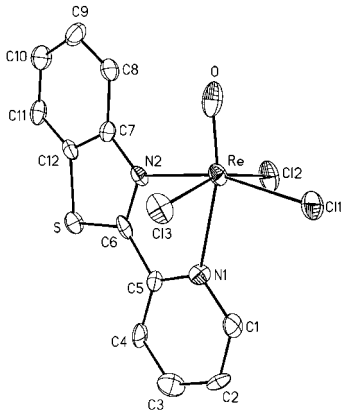

Figure 2. Molecular view and atom-labeling scheme for $ReOCl_3(pbt)$. All non-hydrogen atoms are represented by 30% thermal probability ellipsoids.

Table 1. Selected Bond Distances (Å) and Angles (deg) for $ReOCl_3(pbt)$

	Distances		
Re−O	1.607(9)	Re−Cl(1)	2.291(5)
Re−N(1)	2.270(13)	Re−Cl(2)	2.312(5)
Re−N(2)	2.118(12)	Re−Cl(3)	2.330(5)
	Angles		
O−Re−N(2)	92.8(5)	O−Re−N(1)	165.3(5)
N(2)−Re−N(1)	73.3(5)	O−Re−Cl(1)	104.7(4)
N(2)−Re−Cl(1)	162.3(4)	N(1)−Re−Cl(1)	89.4(4)
O−Re−Cl(2)	101.2(5)	N(2)−Re−Cl(2)	86.4(4)
N(1)−Re−Cl(2)	82.9(4)	Cl(1)−Re−Cl(2)	87.4(2)
O−Re−Cl(3)	96.3(5)	N(2)−Re−Cl(3)	92.9(4)
N(1)−Re−Cl(3)	80.1(4)	Cl(1)−Re−Cl(3)	88.1(2)
Cl(2)−Re−Cl(3)	162.4(2)		

A molecular view of $ReOCl_3(pbt)$ is shown in Figure 2, and selected bond parameters are listed in Table 1. On going from the free ligand (Figure 1) to the complex, the conformation of pbt has changed corresponding to a ∼180° rotation around the C−C bond linking the pyridyl and thiazole rings. With this change the ligand achieves N,N-chelation as in **1**. The coordination chemistry of pbt has received some previous attention.[13]

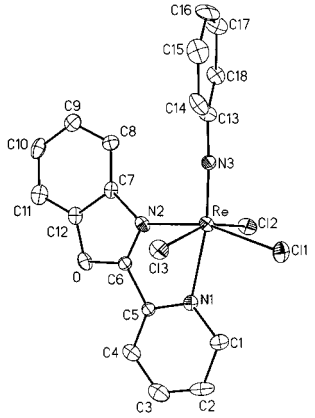

Figure 3. Molecular view and atom-labeling scheme for $Re(NPh)Cl_3(pbo)$. All non-hydrogen atoms are represented by 30% thermal probability ellipsoids.

The Re(pbt) fragment in $ReOCl_3(pbt)$ is planar with a mean deviation of 0.05 Å, and the oxo oxygen atom also lies in this plane. There is a relatively short nonbonded C8···O contact, 2.980(3) Å. In the lattice the Re(pbt) fragments align nearly parallel to one another in an infinite array, and this stacking leads to nonbonded Cl···S contacts (3.475(2) and 3.421(2) Å) involving two *trans* chloride ligands and the thiazole S atoms.

In the distorted octahedral $ReOCl_3N_2$ coordination sphere of the complex, the chloride ligands are meridionally disposed. These together with the N(2) atom constitute a plane (mean deviation 0.01 Å) from which the metal atom is displaced 0.27 Å toward the oxo oxygen atom. At 1.607-(9) Å, the Re−O distance is relatively short. In reported $Re^{V}O$ species the Re−O distances generally lie within the range 1.68 ± 0.03 Å, and shorter lengths are uncommon.[14] The Re−N(1) bond is subject to the *trans* influence of the oxo oxygen atom and is accordingly longer than the Re−N(2) bond (*trans* ligand Cl(1)) by ∼0.15 Å.

The structure of $Re(NPh)Cl_3(pbo)$, shown in Figure 3, authenticates N,N-chelation of the new pbo ligand in the planar Re(pbo) fragment. Selected bond parameters are listed in Table 2. In the meridional $ReCl_3N_3$ coordination sphere the metal atom is displaced by 0.36 Å toward the imide nitrogen, N(3), from the plane defined by Cl(1), Cl(2), Cl-(3), and N(2). The observed Re−N(3) length, 1.698(9) Å, corresponds to triple bonding.[15]

Rates and Activation Parameters of Oxygen Atom Transfer. The variable-temperature rates of the reaction of eq 2 (R = Ph) have been studied spectrophotometrically in

(13) (a) Chia P. S. K.; Livingstone, S. E. *Inorg. Chim. Acta* **1968**, *2*, 427. (b) Lindoy, L. F.; Livingstone, S. E. *Inorg. Chim. Acta* **1968**, *2*, 119. (c) Hossain, M.; Chattopadhyay, S. K.; Ghosh, S. *Polyhedron* **1997**, *16*, 143. (d) Maji, M.; Sengupta, P.; Chattopadhyay, S. K.; Mostafa, G.; Schwalbe, C. H.; Ghosh, S. *J. Coord. Chem.* **2001**, *54*, 13.

(14) (a) Mayer, J. M. *Inorg. Chem.* **1988**, *27*, 3899. (b) Edwards, L. F.; Griffith, W. P.; White, A. J. P.; Williams, D. J. *J. Chem. Soc., Dalton Trans.* **1992**, 957.

(15) (a) Dirghangi, B. K.; Menon, M.; Banerjee, S.; Chakravorty, A. *Inorg. Chem.* **1997**, *36*, 3595. (b) Banerjee, S.; Dirghangi, B. K.; Menon, M.; Pramanik, A.; Chakravorty, A. *J. Chem. Soc., Dalton. Trans.* **1997**, 2149. (c) Goeden, G. V.; Haymore, B. L. *Inorg. Chem.* **1983**, *22*, 157. (d) Nugent, W. A.; Haymore, B. L. *Coord. Chem. Rev.* **1980**, *31*, 123.

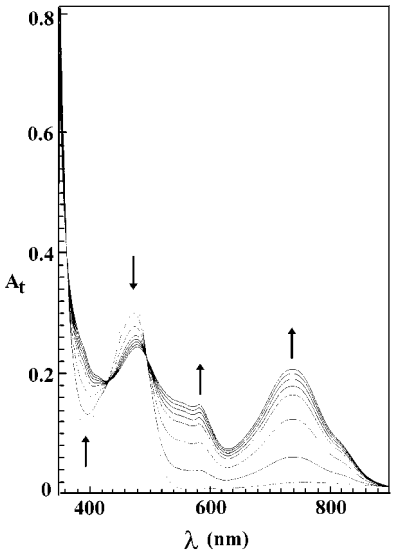

Figure 4. Time evolution spectra for the reaction between $ReOCl_3$(pbo) and PPh_3 in dichloromethane solution at 302 K (A_t is absorbance).

Table 2. Selected Bond Distances (Å) and Angles (deg) for $Re(NPh)Cl_3$(pbo)

	Distances		
Re−N(1)	2.266(9)	Re−Cl(1)	2.324(3)
Re−N(2)	2.075(10)	Re−Cl(2)	2.365(3)
Re−N(3)	1.698(9)	Re−Cl(3)	2.324(3)
	Angles		
N(3)−Re−N(2)	98.4(4)	N(3)−Re−N(1)	170.7(4)
N(2)−Re−N(1)	73.4(3)	N(3)−Re−Cl(1)	99.7(3)
N(2)−Re−Cl(1)	161.7(3)	N(1)−Re−Cl(1)	88.3(2)
N(3)−Re−Cl(3)	102.3(3)	N(2)−Re−Cl(3)	90.0(3)
N(1)−Re−Cl(3)	82.5(3)	Cl(1)−Re−Cl(3)	88.31(12)
N(3)−Re−Cl(2)	95.5(3)	N(2)−Re−Cl(2)	87.7(3)
N(1)−Re−Cl(2)	80.0(3)	Cl(1)−Re−Cl(2)	88.39(12)
Cl(3)−Re−Cl(2)	162.23(11)		

Table 3. Rate Constants and Activation Parameters[a] for the Reaction $ReOCl_3$(pbo) + PPh_2R → $Re(OPPh_2R)Cl_3$(pbo) in Dichloromethane[b,c]

R	*T*, K	10^2[PPh_2R]	10^5k_{obsd}, s^{-1}	$\mathbf{10}^3k$, M^{-1} s^{-1}
Ph	299	0.63	1.95	3.45(0.02)
		1.06	3.42	
		1.40	4.47	
		2.00	6.70	
	302	0.63	2.40	4.18(0.02)
		1.06	4.33	
		1.40	5.60	
		2.00	8.17	
	305	0.63	3.00	5.42(0.02)
		1.06	5.78	
		1.40	7.32	
		2.00	10.53	
	308	0.63	3.73	7.12(0.02)
		1.06	6.95	
		1.40	9.55	
		2.00	13.47	
Me	302	0.61	15.78	24.80(0.05)
		1.15	25.37	
		1.60	34.52	
		2.00	49.62	

[a] For R = Ph, $\Delta H^{\ddagger} = 13.49$ (0.81) kcal mol^{-1} and $\Delta S^{\ddagger} = -24.15(2.5)$ eu. [b] The initial concentration of $ReOCl_3$(pbo) is 1.25×10^{-4} M. [c] Least-squares deviations are given in parentheses.

CH_2Cl_2 solution for both $ReOCl_3$(pbo) and $ReOCl_3$(pbt). Time evolution spectra are characterized by multiple isosbestic points, and a representative case is shown in Figure 4.

Table 4. Rate Constants and Activation Parameters[a] for the Reaction $ReOCl_3$(pbt) + PPh_2R → $Re(OPPh_2R)Cl_3$(pbt) in Dichloromethane[b,c]

R	*T*, K	10^2[PPh_2R]	10^5k_{obsd}, s^{-1}	$\mathbf{10}^3k$, M^{-1} s^{-1}
Ph	299	0.63	0.96	1.68(0.03)
		1.06	1.82	
		1.40	2.18	
		2.00	2.95	
	302	0.63	1.22	2.00(0.06)
		1.06	2.15	
		1.40	2.77	
		2.00	3.87	
	305	0.63	1.51	2.58(0.05)
		1.06	2.71	
		1.40	3.67	
		2.00	5.07	
	308	0.63	2.03	3.35(0.04)
		1.06	3.43	
		1.40	4.72	
		2.00	6.63	
Me	302	0.61	6.70	10.65(0.03)
		1.15	13.30	
		1.60	17.15	
		2.00	21.91	

[a] For R = Ph, $\Delta H^{\ddagger} = 14.31(0.56)$ kcal mol^{-1} and $\Delta S^{\ddagger} = -23.32(1.8)$ eu. [b] The initial concentration of $ReOCl_3$(pbt) is 1.25×10^{-4} M. [c] Least-squares deviations are given in parentheses.

Under pseudo-first-order conditions (excess PPh_3), the rates are proportional to the concentration of the oxo complex and the observed rate constant, k_{obsd}, is proportional to the concentration of PPh_3. The reaction law is thus second order, eq 4

$$\text{rate} = k_{obsd}[ReOCl_3(L)] = k[ReOCl_3(L)][PPh_3] \quad (4)$$

(L = pbo/pbt). The rate constant k follows the Eyring equation. Rate data and activation parameters are listed in Tables 3 and 4. The large and negative entropy of activation implies close association of $ReOCl_3(L)$ and PPh_3 in the transition state. The probable mode of this association and subsequent events are stylized in **4** in light of previous work[3]

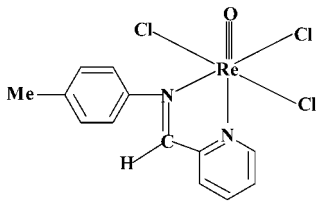

$ReOCl_3$(pal)

5

and the findings on oxygen atom transfer reactions of $Mo^{VI}O_2$ and $W^{VI}O_2$ species.[16] In **4** the full and broken lines, respectively, represent coordinate covalent bonds and weak links. Following attack on π^*(ReO) orbitals by the phosphine lone pair (**4a**), the π-bonds are weakened and a O···P link is established (**4b**, transition state). In the end, the P═O bond remains coordinated to the metal (**4c**). In $Re(OPPh_3)Cl_3$(pbt),

(16) (a) Tucci, G. C.; Donahue, J. P.; Holm, R. H. *Inorg. Chem.* **1998**, *37*, 1602 and references therein. (b) Pietsch, M. A.; Hall, M. B. *Inorg. Chem.* **1996**, *35*, 1273. (c) Enemark, J. H.; Young, C. G. *Adv. Inorg. Chem.* **1993**, *43*, 1.

the P atom lies ~2.8 Å away from the centroids of the two OCl_2 faces. The distances from the OClN centroids are ~3.3 Å. Thus, phosphine attack may have occurred from the side away from the chelate ring.

Reactivity Trends. In reaction model **4**, an increase of the phosphine basicity should make the reaction more facile. In agreement with this, PPh_2Me reacts faster than PPh_3, the ratio $k(PPh_2Me)/k(PPh_3)$ being 5.93 (L = pbo) and 5.33 (L = pbt) at 302 K (Tables 3 and 4). The data of Tables 3 and 4 also reveal that $ReOCl_3$(pbo) is a more potent transfer reagent than $ReOCl_3$(pbt), the rate constant for the former complex at any given temperature being approximately double that of the latter complex. This is qualitatively consistent with the heteroatom electronegativity order O > S, resulting in larger electron withdrawl from the oxometal moiety in the pbo complex. Significantly, for protonated azoles the pK_a trend is oxazole < thiazole.[17]

In similarly constituted molecules, the metal reduction potential is a qualitative index of the effective electron density at the metal site (the higher the $E_{1/2}$, the lower the electron density). In acetonitrile solution the $Re^{V}O$ complexes display a quasireversible (peak-to-peak separation ~100 mV) one-electron response assigned to the $Re^{VI}O/Re^{V}O$ couple. The $E_{1/2}$ values are 1.64 and 1.54 V vs SCE at 298 K for the pbo and pbt complexes, respectively. Significantly, the Re^{VI}-NPh/Re^{V}NPh couple in **3** also displays a similar trend: 0.85 V (pbo) and 0.81 V (pbt). Oxygen atom transfer rate and $E_{1/2}$ data for a $Re^{V}O$ pyridylaldimine system, viz., $ReOCl_3$(pal), **5**, are also available.[3] Complex **5** ($k = 7.96 \times 10^{-3}$ M^{-1} s^{-1} at 299 K) reacts with PPh_3 more than twice as fast as $ReOCl_3$(pbo). The $Re^{VI}O/Re^{V}O$ reduction potential of **5** is also relatively high, 1.72 V.[3] Indeed the $E_{1/2}$ and ln k values of the three complexes are linearly related with a correlation constant of 0.999 (Figure 5).

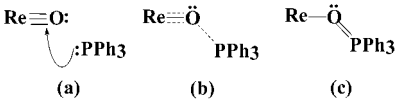

4

Last, we note that the Re−O distance in $ReOCl_3$(pbt) is 0.06 Å shorter than that in $ReOCl_3$(pal).[3] The superior strength of the metal−oxo bond (less stable π^*(ReO) orbitals) in the pbt complex would hinder transfer of the oxygen atom by weakening the association in the activated state. Indeed the $\Delta H^{\ddagger}$ value of $ReOCl_3$(pbt) is more positive and the $\Delta S^{\ddagger}$ value is less negative (Table 4) than those of $ReOCl_3$(pal) ($\Delta H^{\ddagger} = 8.91$ kcal M^{-1} s^{-1} and $\Delta S^{\ddagger} = -38.69$ eu).[3] Thus, the relatively higher electron density of the Re−O bond in the pbt complex as reflected in the smaller $E_{1/2}$ value (see above) is also expressed as a shortening of the Re−O bond with the consequent sluggishness of the oxygen atom transfer reaction.

Concluding Remarks

Oxorhenium(V) complexes of two pyridyl heterocyclic ligands have been isolated in the form of $Re^{V}OCl_3$(pbo) and $Re^{V}OCl_3$(pbt) from which the corresponding $Re^{III}(OPPh_2R)$ and Re^{V}(NPh) species have been prepared. The reactions are stereoretentive, the $ReCl_3$ moeity being uniformly meridional in geometry. The azole ligands are N,N-chelated, and in the case of pbt, chelation is attended with a conformational change.

The associative oxygen atom transfer reactions of $ReOCl_3$(pbo), $ReOCl_3$(pbt), and $ReOCl_3$(pal)[3] with tertiary phosphines are consistent with reaction model **4**. The rate constants increase with phosphine basicity (PPh_3 < PPh_2Me), azole heteroatom electronegativity (S(pbt) < O(pbo)), metal reduction potential (**1** (X = S) < **1** (X = O) < **5**), and metal−oxo bond length (**1** (X = S) < **5**). A linear correlation between metal reduction potentials and the logarithmic rate constants is noted.

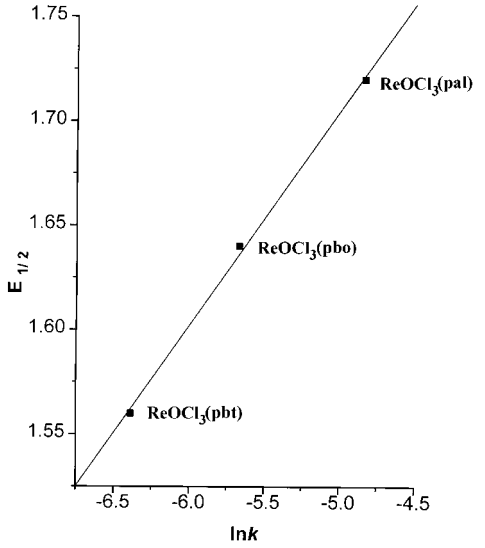

Figure 5. $Re^{VI}O/Re^{V}O$ reduction potential versus logarithmic rate constant for oxygen atom transfer to PPh_3 at 299 K.

Experimental Section

Materials. The $ReOCl_3(PPh_3)_2$ complex was prepared by a reported method.[18] The purification and drying of dichloromethane and acetonitrile for synthesis as well as electrochemical and spectral work were done as before.[19] Benzene was distilled over sodium before use. All other chemicals and solvents were of reagent grade and were used as received.

Physical Measurements. All UV−vis spectral measurements were carried out with a Shimadzu UVPC 1601 spectrometer fitted with thermostated cell compartments. Proton NMR spectra were recorded on a Bruker FT 300 MHz spectrometer. The atom numbering scheme used for ^{1}H NMR is the same as in crystallography. Spin−spin structures are abbreviated as follows: s, singlet; d, doublet; t, triplet; i, ill-resolved. Electrochemical measurements were performed on a PAR model 370-4 electrochemistry system as described elsewhere[20] using a platinum working electrode under a nitrogen atmosphere. The supporting electrolyte was tetraethy-

(17) Katritzsky, A. R.; Rees, C. W. *Comprehensive Heterocyclic Chemistry*, 1st ed.; Pergamon Press: New York, 1984; Vol. 6, p 184.

(18) Chatt, J.; Rowe, G. A. *J. Chem. Soc.* **1962**, 4019.

(19) (a) Lahiri, G. K.; Bhattacharya, S.; Ghosh, B. K.; Chakravorty, A. *Inorg. Chem.* **1987**, *26*, 4324. (b) Sawyer, D. T.; Roberts, J. L., Jr. *Experimental Electrochemistry for Chemists*; Wiley: New York, 1974; p 167.

(20) Pramanik, A.; Bag, N.; Lahiri, G. K.; Chakravorty, A. *Inorg. Chem.* **1991**, *30*, 410.

lammonium perchlorate (TEAP), and potentials are referred to the saturated calomel electrode (SCE) without junction correction. Room-temperature magnetic susceptibilities of powders were measured with a model 155 PAR vibrating sample magnetometer. Microanalyses (C, H, N) were performed using a Perkin-Elmer 2400 series II elemental analyzer.

Preparation of Ligands. a. 2-(2-Pyridyl)benzoxazole, pbo. Pyridine-2-carboxaldehyde (1.07 g, 10 mmol) and 2-aminophenol (1.09 g, 10 mmol) were mixed thoroughly to make a paste which was then extracted thrice (3 × 15 mL) with diethyl ether. The Schiff base was isolated as a red-yellow solid by removing the solvent from the extract. To a solution of the Schiff base (0.99 g, 5 mmol) in 50 mL of dichloromethane was added silver oxide (1.74 g, 7.5 mmol), and the mass was magnetically stirred for 10 h in the air and then filtered through a Celite bed. The filtrate was then subjected to chromatography on an active alumina column (30 × 1 cm). A pale-yellow band was eluted by benzene, and solvent removal from the eluate under reduced pressure afforded pbo as a pale-yellow solid which was dried in vacuo over fused $CaCl_2$. The solid was recrystallized from hot methanol, furnishing pale-yellow needles. Yield: 0.75 g (77% based on the Schiff base). Mp: 102 °C. Anal. Calcd for $C_{12}H_8N_2O$: C, 73.46; H, 4.11; N, 14.28. Found: C, 73.44; H, 4.08; N, 14.30. UV−vis (λ_{max}, nm (ϵ, M^{-1} cm^{-1}), CH_2Cl_2 solution): 250 (28500); 305 (22950). ^{1}H NMR (δ (*J*, Hz), $CDCl_3$): 8.74 (H(1), d, 4.7); 7.59 (H(2), t, 4.6); 7.76 (H(3), t, 6.8); 7.82 (H(4), d, 6.2); 8.28 (H(8), d, 7.9); 7.33 (H(9), t, 5.6); 7.30 (H(10), t, 5.2); 7.38 (H(11), d, 5.9).

b. 2-(2-Pyridyl)benzthiazole, pbt. To a solution of pyridine-2-carboxaldehyde (1.07 g, 10 mmol) in 20 mL of methanol was added 2-aminothiophenol (1.25 g, 10 mmol). The solution was refluxed for 6 h in the air. Upon cooling of the solution to room temperature, a light-yellow solid precipitated. The solid was collected by filtration and washed several times with hexane and then with diethyl ether. It was finally dried in vacuo over fused $CaCl_2$. The solid was recrystallized from hot methanol, affording pale-yellow needles. Yield: 1.76 g (82%). Mp: 132 °C. Anal. Calcd for $C_{12}H_8N_2S$: C, 67.90; H, 3.80; N, 13.20. Found: C, 67.86; H, 3.76; N, 13.23. UV−vis (λ_{max}, nm (ϵ, M^{-1} cm^{-1}), CH_2Cl_2 solution): 312 (35105); 234 (29030). ^{1}H NMR (δ (*J*, Hz), $CDCl_3$): 8.68 (H(1), d, 4.6); 7.51 (H(2), t, 7.5); 7.85 (H(3), t, 7.5); 8.10 (H(4), d, 8.1); 8.37 (H(8), d, 7.8); 7.42 (H(9), t, 7.9); 7.38 (H(10), t, 6.2); 7.96 (H(11), d, 7.7).

Preparation of Complexes. a. $ReOCl_3$(pbo). To a suspension of $ReOCl_3(PPh_3)_2$ (100 mg, 0.12 mmol) in 50 mL of benzene was added 24 mg (0.12 mmol) of pbo. The resulting mass was stirred magnetically for 4.5 h at room temperature, affording a turbid yellow solution which was kept undisturbed overnight at 0 °C, to ensure complete precipitation. The yellow solid was collected by filtration, washed thoroughly with benzene, and finally dried in vacuo over fused $CaCl_2$. Yield: 36 mg (58%). Anal. Calcd for $C_{12}H_8Cl_3N_2O_2Re$: C, 28.53; H, 1.60; N, 5.54. Found: C, 28.51; H, 1.62; N, 5.56. UV−vis (λ_{max}, nm (ϵ, M^{-1} cm^{-1}), CH_2Cl_2 solution): 764 (120); 475 (2350); 318 (16060). ^{1}H NMR (δ (*J*, Hz), DMSO-d_6): 9.55 (H(1), d, 5.4); 7.56 (H(2), t, 6.6); 8.46 (H(3), t, 7.7); 8.20 (H(4), d, 8.7); 8.89 (H(8), d, 7.8); 8.07 (H(9), t, 7.4); 7.94 (H(10), t, 8.4); 8.55 (H(11), d, 6.3).

b. $ReOCl_3$(pbt). This complex was prepared by a similar procedure. Yield: 32 mg (51%). Anal. Calcd for $C_{12}H_8Cl_3N_2SORe$: C, 27.65; H, 1.55; N, 5.37. Found: C, 27.68; H, 1.60; N, 5.31. UV−vis (λ_{max}, nm (ϵ, M^{-1} cm^{-1}), CH_2Cl_2 solution): 766 (240); 493 (2700); 323 (11290). ^{1}H NMR (δ (*J*, Hz), DMSO-d_6): 8.75 (H(1), d, 5.4); 7.57 (H(2), t, 6.4); 8.41 (H(3), t, 7.5); 8.10 (H(4), d, 8.1); 8.55 (H(8), d, 7.8); 7.94 (H(9), t, 7.8); 7.88 (H(10), t, 8.1); 8.50 (H(11), d, 7.5).

c. $Re(OPPh_3)Cl_3$(pbo). To a solution of $ReOCl_3$(pbo) (65 mg, 0.13 mmol) in 25 mL of dichloromethane was added 68 mg (0.28 mmol) of PPh_3. The resulting solution was magnetically stirred for 3.5 h at room temperature, and during this time the solution color changed from yellow to violet. The solution was subjected to chromatography on a silica gel column (25 × 1 cm, 60−120 mesh). Excess PPh_3 was eluted with benzene. The violet band that followed was eluted with a benzene−acetonitrile (50:3) mixture. Solvent removal from the eluate under reduced pressure afforded $Re(OPPh_3)Cl_3$(pbo) as a violet solid. Yield: 70 mg (71%). Anal. Calcd for $C_{30}H_{23}Cl_3N_2O_2PRe$: C, 46.95; H, 3.02; N, 3.65. Found: C, 46.95; H, 3.03; N, 3.67. UV−vis (λ_{max}, nm (ϵ, M^{-1} cm^{-1}), CH_2Cl_2 solution): 733 (2420); 580 (1710); 513 (1950); 319 (11330). ^{1}H NMR (δ (*J*, Hz), $CDCl_3$): 25.85 (H(1), d, 7.8); 7.94 (H(2), t, 8.3); 10.99 (H(3), t, 7.6); 8.37 (H(4), d, 7.8); 20.75(H(8), d, 7.7); 10.36 (H(9), t, 7.6); 6.98 (H(10), t, 6.9); 22.96 (H(11), d, i). ^{1}H NMR (δ (*J*, Hz), PPh_3): 7.45 (H(*o*), d, 5.1); 7.40 (H(*m*), t, i); 7.07 (H(*p*), t, i). μ (in powder): 1.95 μ_B (298 K).

The complex could also be prepared directly from a solution of $ReOCl_3(PPh_3)_2$ (50 mg, 0.06 mmol) in 25 mL of dichloromethane containing pbo (12 mg, 0.06 mmol). Magnetic stirring at room temperature for 3.5 h afforded a violet solution which was subjected to chromatography on a silica gel column as described above.

d. $Re(OPPh_3)Cl_3$(pbt). A similar procedure was used to prepare this and the following phosphine oxide complexes. Yield: 79 mg (75%). Anal. Calcd for $C_{30}H_{23}Cl_3N_2SOPRe$: C, 45.99; H, 2.96; N, 3.58. Found: C, 45.95; H, 2.89; N, 3.61. UV−vis (λ_{max}, nm (ϵ, M^{-1} cm^{-1}), CH_2Cl_2 solution): 737 (4200); 585 (3050); 518 (2940); 328 (21340). ^{1}H NMR (δ (*J*, Hz), $CDCl_3$): 28.24 (H(1), d, 7.8); 8.32 (H(2), t, 7.5); 22.54 (H(3), t, i); 7.83 (H(4), d, 7.5); 23.74 (H(8), d, i); 10.69 (H(9), t, 7.5); 8.35 (H(10), t, 7.8); 12.15 (H(11), d, 7.8). ^{1}H NMR (δ (*J*, Hz), PPh_3): 7.19 (H(*o*), d, 6.9); 6.44 (H(*m*), t, 7.8); 7.04 (H(*p*), t, 7.2). μ (in powder): 2.02 μ_B (298 K).

e. $Re(OPPh_2Me)Cl_3$(pbo). Yield: 67 mg (74%). Anal. Calcd for $C_{25}H_{21}Cl_3N_2O_2PRe$: C, 42.57; H, 3.00; N, 3.97. Found: C, 42.60; H, 2.97; N, 3.95. UV−vis (λ_{max}, nm (ϵ, M^{-1} cm^{-1}), CH_2Cl_2 solution): 733 (2720); 578 (1870); 503 (2180); 316 (11120). ^{1}H NMR (δ (*J*, Hz), $CDCl_3$): 25.45 (H(1), d, 7.2); 2.32 (H(2), t, i); 10.57 (H(3), t, 7.0); −3.53 (H(4), d, 11.6); 10.78 (H(11), d, 6.6); 8.17 (H(9), t, 7.2); 8.59 (H(10), t, 9.4); 21.94 (H(8), d, 7.5). ^{1}H NMR (δ (*J*, Hz), PPh_2Me): 6.09 (H(*o*), d, i); 7.33 (H(*m*), t, 7.4); 7.88 (H(*p*), t, 8.1); −4.45 (Me, s). μ (in powder): 2.08 μ_B (298 K).

f. $Re(OPPh_2Me)Cl_3$(pbt). Yield: 68 mg (73%). Anal. Calcd for $C_{25}H_{21}Cl_3N_2SOPRe$: C, 41.64; H, 2.94; N, 3.89. Found: C, 41.58; H, 2.91; N, 3.96. UV−vis (λ_{max}, nm (ϵ, M^{-1} cm^{-1}), CH_2Cl_2 solution): 741 (4600); 584 (2800); 515 (2650); 328 (18700). ^{1}H NMR (δ (*J*, Hz), $CDCl_3$): 29.15 (H(1), d, 8.0); 9.02 (H(2), t, 7.7); 22.16 (H(3), t, i); 8.47 (H(4), d, 7.8); 22.69 (H(8), d, i); 11.18 (H(9), t, 7.4); 8.72 (H(10), t, 8.7); 13.87 (H(11), d, 7.4). ^{1}H NMR (δ (*J*, Hz), PPh_2Me): 8.01 (H(*o*), d, 8.2); 7.84 (H(*m*), t, 8.2); 7.49 (H(*p*), t, 6.8); −3.43 (Me, s). μ (in powder): 2.05 μ_B (298 K).

g. $Re(NC_6H_5)Cl_3$(pbo). To a solution of $ReOCl_3$(pbo) (60 mg, 0.12 mmol) in dichloromethane (15 mL) was added aniline (56 mg, 0.60 mmol) in toluene (50 mL), and the mixture was heated to reflux for 1.5 h, affording a blue solution. The solvent was then removed under reduced pressure, and the mass thus obtained was subjected to chromatography on a silica gel column (20 × 1 cm, 60−120 mesh). Excess aniline was eluted with benzene. A blue band was then eluted with a benzene−acetonitrile (25:1) mixture. Solvent removal from the eluate under reduced pressure afforded $Re(NC_6H_5)Cl_3$(pbo) as a blue solid. Yield: 56 mg (81%). Anal. Calcd for $C_{18}H_{13}Cl_3N_3ORe$: C, 37.26; H, 2.26; N, 7.24. Found: C, 37.30; H, 2.28; N, 7.22. UV−vis (λ_{max}, nm (ϵ, M^{-1} cm^{-1}), CH_2Cl_2

Table 5. Crystallographic Data for pbt, $ReOCl_3$(pbt), and $Re(NPh)Cl_3$(pbo)

	pbt	$ReOCl_3$(pbt)	$Re(NPh)Cl_3$(pbo)
empirical formula	$C_{12}H_8N_2S$	$C_{12}H_8Cl_3N_2OSRe$	$C_{18}H_{13}Cl_3N_3ORe$
fw	212.28	520.81	579.86
cryst size, mm	0.40 × 0.40 × 0.30	0.35 × 0.30 × 0.30	0.40 × 0.35 × 0.30
cryst syst	orthorhombic	monoclinic	monoclinic
space group	$Pca2_1$	$P2_1/c$	$P2_1/c$
a, Å	13.762(9)	11.174(7)	9.566(6)
b, Å	12.952(8)	16.403(10)	16.082(8)
c, Å	11.077(4)	7.751(2)	11.841(5)
α, deg			
β, deg		99.35(4)	94.03(4)
γ, deg			
V, Å	1974(2)	1401.8(13)	1817(2)
Z	8	4	4
ρ_{calcd}, mg m^{-3}	1.428	2.468	2.120
μ, mm^{-1}	0.289	9.382	7.141
R1,[a] wR2[b] [$I > 2\sigma(I)$]	0.0543, 0.1354	0.0553, 0.1308	0.0581, 0.1497

[a] $R1 = \sum||F_o| - |F_c||/\sum|F_o|$. [b] $wR2 = [\sum w(F_o^2 - F_c^2)^2/\sum w(F_o^2)^2]^{1/2}$.

solution): 735 (330); 563 (1900); 320 (10600). ^{1}H NMR (δ (J, Hz), $CDCl_3$): 9.48 (H(1), d, 5.2); 7.16 (H(2), t, 8.0); 8.12 (H(3), t, 6.6); 8.47 (H(4), d, 7.9); 8.58 (H(8), d, 4.8); 7.90 (H(9), t, 4.7); 7.85 (H(10), t, 6.5); 7.38 (H(11), d, 8.4). ^{1}H NMR (δ (J, Hz), NC_6H_5): 7.74 (H(o), d, 8.2); 7.51 (H(m), t, 4.0); 7.65 (H(p), t, 4.6).

h. $Re(NC_6H_5)Cl_3$(pbt). A procedure similar to the above was used. Yield: 63 mg (79%). Anal. Calcd for $C_{18}H_{13}Cl_3N_3SRe$: C, 36.25; H, 2.20; N, 7.05. Found: C, 36.31; H, 2.18; N, 7.07. UV−vis (λ_{max}, nm (ϵ, M^{-1} cm^{-1}), CH_2Cl_2 solution): 738 (270); 566 (1840); 321 (10730). ^{1}H NMR (δ (J, Hz), $CDCl_3$): 9.43 (H(1), d, 5.4); 7.22 (H(2), t, 6.6); 8.07 (H(3), t, 7.8); 7.96 (H(4), d, 8.1); 7.89 (H(8), d, 7.8); 7.81 (H(9), t, i); 7.78 (H(10), t, 4.3); 7.63 (H(11), d, 6.8). ^{1}H NMR (δ (J, Hz), NC_6H_5): 7.71 (H(o), d, 7.4); 7.42 (H(m), t, 8.2); 7.50 (H(p), t, 7.6).

Rate Measurements. The representative case of the reaction of $ReOCl_3$(pbo) with PPh_3 will be described. A known excess of PPh_3 was added to a solution of $ReOCl_3$(pbo) (1.25×10^{-4} M) in dichloromethane at the desired temperature, and the thermostated reaction was followed spectrophotometrically (quartz cell path length 1 cm) by measuring the absorbance (A_t) of the peak at 737 nm as a function of time (t). The absorbance (A_α) at the end of the reaction (24 h) was also measured. Values of k_{obsd} and k were obtained from the slopes of the linear plots of $-[\ln(A_\alpha - A_t)]$ versus t and k_{obsd} versus [PPh_3], respectively. The activation enthalpy and entropy parameters were determined from the linear plot of $-(\ln kh)/K_BT$ vs T^{-1} using the Eyring equation (eq 5).

$$k = (K_BT/h)[\exp(-\Delta H^{\ddagger}/RT)\exp(\Delta S^{\ddagger}/R)] \quad (5)$$

X-ray Structure Determination. Crystals of pbt and $ReOCl_3$(pbt) were grown by slow evaporation of methanol and dichloromethane solutions, respectively. In the case of $Re(OPPh_3)Cl_3$(pbt) and $Re(NPh)Cl_3$(pbo), slow diffusion of hexane into dichloromethane solution afforded single crystals. Cell parameters were determined by a least-squares fit of 30 machine-centered reflections ($14° \le 2\theta \le 28°$). Data were collected by the ω scan technique in the 2θ range 3−50° for pbt, $ReOCl_3$(pbt), and $Re(OPPh_3)Cl_3$(pbt) and in the 2θ range 3−47° for $Re(NPh)Cl_3$(pbo) on a Siemens R3m/V four-circle diffractometer with graphite-monochromated Mo Kα ($\lambda = 0.71073$ Å) radiation at 298 K. Two check reflections after each 198 reflections showed no significant intensity reduction for any of the crystals. Data were corrected for Lorentz-polarization effects and in the case of complexes for absorption.[21]

The structure of pbt was generated by direct methods and those of $ReOCl_3$(pbt), $Re(OPPh_3)Cl_3$(pbt), and $Re(NPh)Cl_3$(pbo) by using Patterson maps followed by successive Fourier synthesis. The structures of pbt, $ReOCl_3$(pbt), and $Re(NPh)Cl_3$(pbo) were refined by full-matrix least-squares procedures on F^2. All non-hydrogen atoms were made anisotropic, and the hydrogen atoms were added at the calculated positions. Calculations were performed using the SHELXTL V5.03[22] program package. The crystal data for pbt, $ReOCl_3$(pbt), and $Re(NPh)Cl_3$(pbo) are given in Table 5.

The complex $Re(OPPh_3)Cl_3$(pbt) crystallized in the chiral space group $P1$ with $Z = 2$, and the asymmetric unit generated from Patterson maps and successive Fourier synthesis consisted of two molecules making a nearly centrosymmetric pair. This vitiated least-squares refinement. Only the coordination sphere could be refined anisotropically, the benzene rings having been affixed as idealized hexagons. With these constraints the refinement did not proceed normally, but the gross structure was revealed with certainty. Crystal data are as follows: empirical formula $C_{30}H_{23}Cl_3N_2OPSRe$, formula weight 783.08, crystal system triclinic, space group $P1$, $a = 10.369(8)$ Å, $b = 11.459(6)$ Å, $c = 13.787(5)$ Å, $\alpha = 91.08(4)°$, $\beta = 89.92(5)°$, $\gamma = 106.98(5)°$, $V = 1566(2)$ Å^3, $Z = 2$, $R1[I > 2\sigma(I)] = 0.1070$, $wR2[I > 2\sigma(I)] = 0.2527$. Selected bond lengths probably good to within ±0.05 Å are Re−O 2.08 Å, Re−Cl 2.31 Å, and O = P 1.50 Å, which are not incompatible with those in other Re^{III}−OP systems.[1−3] All other results are deposited.

Acknowledgment. We thank the Department of Science and Technology and Council of Scientific and Industrial Research, New Delhi, for financial support.

Supporting Information Available: For pbt, $ReOCl_3$(pbt), $Re(OPPh_3)Cl_3$(pbt), and $Re(NPh)Cl_3$(pbo), crystallographic data (atomic coordinates and equivalent isotropic coefficients, complete bond distances and angles, anisotropic thermal parameters, and hydrogen atom positional parameters) and crystallographic files in CIF format. This material is available free of charge via the Internet at http://www.pubs.acs.org.

IC011064T

(21) North, A. C. T.; Philips, D. C.; Mathews, F. S. *Acta Crystallogr.* **1968**, *24A*, 351.
(22) Sheldrich, G. M. *SHELXTL V5.03*; Bruker Analytical X-ray Systems: Madison, WI, 1994; Part Number 269-015900.